EFFECT OF LEVEE AND CHANNEL STRUCTURES ON LONG LAVA FLOW EMPLACEMENT: MARTIAN EXAMPLES FROM THEMIS AND MOLA DATA. M.N. Peitersen[1] , J.R. Zimbelman[2], P. R. Christensen[3], J. W. Rice[3] and C. Bare[4], [1]Ares Consulting, 2128 Rockwell Avenue, Catonsville, MD, 21228; matthew.peitersen@verizon.net, [2]CEPS/NASM MRC 315, Smithsonian Institution, Washington, DC 20560; jrz@nasm.si.edu, Dept. of Geology, Arizona State Univ., Tempe, AZ 85287-1404, [4]GEST/MOLA Science Team, GSFC, Greenbelt, MD, 20771.

Introduction: Long lava flows (discrete flow units with lengths exceeding 50 km) are easily identified features found on many planetary surfaces. An ongoing investigation [1-7] is being conducted into the origin of these flows. Here, we limit our attention to long lava flows which show evidence of channel-like structures.

Presence of channels in some long lava flows: Channels and channel-like structures (e.g., collapsed lava tubes) have been identified on some long lava flows [1, 8] and may be present but undetected on others. Improved techniques and imagery (e.g. MOLA, THEMIS) may identify additional channels [c.f. 7-9], and will allow improved mapping of these structures and the related flow margins. [10] In this study, we examine the potential effects of channels and levee building on flow emplacement. Strong correlations between flow morphology (particularly changes in width) and the presence or absence of levees have been demonstrated in previous studies [11-14] and can be clearly seen in Fig. 1.

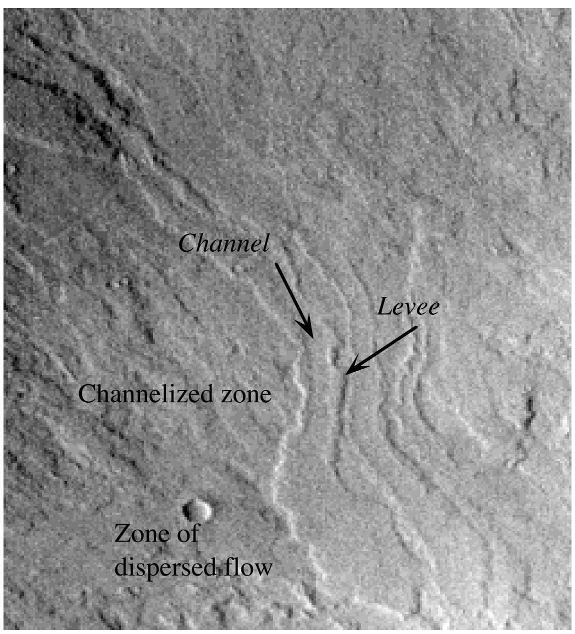

Figure 1. Evidence for correlation between levees and flow morphology. Olympus Mons flow widens as lava escapes from channelized zone into zone of dispersed flow. Subscene from Viking orbiter Image 468S34. North is to upper left; image is ~20 km from top to bottom. Flow margins and levee and channel structures are marked.

Effects of channels and levees on the emplacement of lava flows: When considering the potential effects of channel and levee structures on flow emplacement, two possibilities immediately present themselves. Levees may insulate the flowing lava; they also direct/channel it. With lateral spreading inhibited by the levees, more volume is fed to the active flow front. If the levees also reduce meandering, the channeled flow will have less surface area for the same length, reducing cooling. These mechanisms should increase potential flow length, by increasing supply and decreasing cooling. Working against this, the construction of levees takes material away from the flow front.

Rheological Modeling of Lava Flows: A standard approach to lava flow modeling attempts to use flow geomorphometric measurements (e.g. width, thickness, underlying slope) to estimate rheological parameters (e.g. yield strength, viscosity); this allows constraints to be placed on flow properties (e.g. composition, volatile content) and emplacement conditions [15-16]. Effective use of these models requires accurate flow margin discrimination; measurement of deposits whose dimensions reflect that of the active lava is most appropriate. Thus, sufficient image resolution is mandatory. In the theoretical example illustrated (Fig. 2), failure to identify the flow channel on low-resolution images results in its interpretation as a simple lobe of uniform dimensions, implying no change in rheology. When high resolution data allows the channel to be mapped, the models are most appropriately applied to the active lava (the channel and the lobe), indicating a substantial change in rheology. A flow model which takes into account the effects of channels and levees is described below.

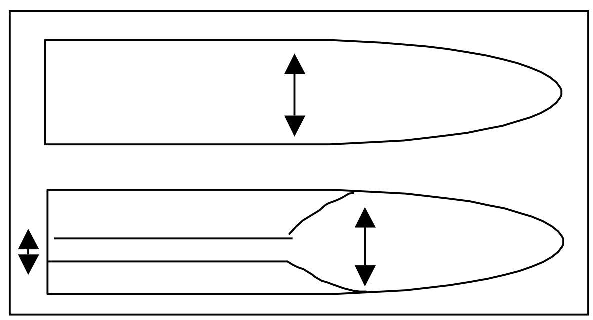

Figure 2. One lava flow, two interpretations. Lacking images sufficient to resolve the channel, the interpreter measures a relatively constant flow width, implying no rheological changes. When channel can be mapped, the active lava changes width dramatically over the length of the flow.

The steady-state model: We begin our investigation of channelized flows by assuming a steady-state condition, where an active lava channel feeds a zone of dispersed flow (the "lobe"). For the purposes of this initial discussion, we ignore the effects of levee-building, and assume no volume loss between channel and lobe. Applying flow continuity, we can solve for a relation comparing the flow velocities between any two points along the flow, in terms of flow dimensions: $\mathbf{v_2/v_1 = A_1/A_2}$, where v = velocity and A = cross-sectional area of the active part of the flow. For the simple bimodal system illustrated in Fig. 2, if we make the simplifying assumption that the depth in the channel of the flow equals the thickness of the lobe, the channel/lobe velocity ratio becomes the inverse ratio of flow widths, and the abrupt change in velocity as the flow exits the channel indicates a change in either driving force (slope) or rheology at this point. By selecting an appropriate form, we can relate flow dimensions to rheological parameters. For Newtonian rheology, we can obtain a relationship describing how viscosity at any point x compares to the initial reference point: **□(x)/□(0) = 1/□(x) (h(x)/h(0))^3 (w(x)/(w(0)) (sin □(x)/sin □(0),** where □ = Newtonian viscosity, g = gravitational acceleration, h = flow thickness, w = flow width, and □ = underlying slope. For the simple channeled flow (Fig. 2), viscosity can clearly be demonstrated as substantially lower in the channel; thus the presence of these channels may be crucial to the flow obtaining great length. To constrain this model realistically, accurate flow images are essential. Widths can be easily obtained from Viking images (Fig. 1), as can thicknesses and channel depths when sufficient shadows are available, but flow channels may be more clearly differentiated in higher-resolution THEMIS images (Fig. 3). Dimensions may also be obtained from MOLA profiles (Fig. 4), provided the channels are of sufficient size to be resolved.

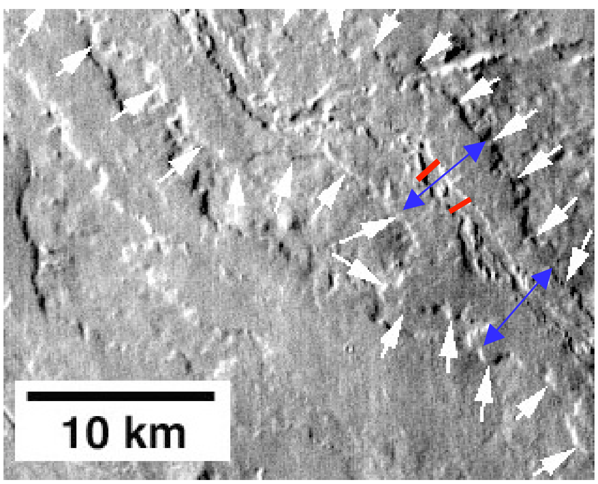

Figure 3. Using THEMIS images to constrain flow and channel widths. White arrows point to flow margins, blue mark flow widths, and red bars denote channel widths. Subscene modified from THEMIS image no. I02700002, 100 m/pixel original resolution, approximate center 7.8° N, 249.5° E.

The mass-loss model: We now consider the effect of levee-building processes, which divert volume from the active part of the flows, by inserting a "retention factor" □ (x), the fraction of supply remaining in the active flow from the reference position (0) to the measured position (x), in the previous equation: **□(x)/□(0) = 1/□(x) (h(x)/h(0))^3 (w(x)/(w(0)) (sin □(x)/sin □(0).** Where flow is constant, □ = 1. Loss to levees will result in □ decreasing downflow. (The effects of inflation could also be considered with an increasing □). Under this condition, given constant slopes and flow dimensions, viscosity will increase As previous studies [4, 16] have shown that estimates of viscosity are far more dependent on the amount of mass loss than on the form of rheology assumed, accurate measurement of flow levee dimensions (to constrain □)are crucial to constraining □. Baloga et al. used a similar approach for Hawaiian flows at Puu Oo [16]; as the extent of the levees was not mapped, they were forced to assume a mass-loss function where levee building continued throughout the period of emplacement. By use of their "volume-loss" model, they obtained rapidly increasing viscosity estimates from relatively uniform flow dimensions; such flows would presumably not obtain long lengths. If, however, levee building ceases at some point prior to flow cessation, as has been observed in the field [17], the active part of the flow may retain more of the volume, and levees may serve principally to direct and insulate flows, allowing greater lengths to be reached than the flows would otherwise obtain.

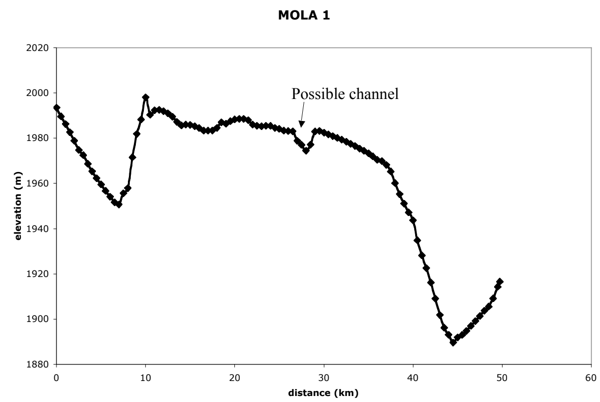

Figure 4. MOLA profile across flow, used to constain flow and channel dimensions. The data is from the same flow illustrated in Fig. 3, but taken at a different location.

Work in progress: Currently, regridded high-resolution MOLA data are being used in conjunction with THEMIS images. By mapping out the location and extent of channel and levee structures in Martian flows, we hope to provide realistic constraints for flow rheology modeling.

References: [1] J.R. Zimbelman (1998), *JGR, 103,* 27,503-27516. [2] M.N. Peitersen and J.R. Zimbelman (2000), *EOS, 81, Abstracts Spring AGU*, S297. [3] M.N. Peitersen et al. (2002), *LPS XXXIII,* Abs. #1026. [4] M.N. Peitersen et al. (2002), *EOS, 83, Abstracts Spring AGU*, S222. [5] M.N. Peitersen et al. (2002), *EOS, 83, Abstracts Fall AGU, P71B-0458, F831*. [6] J.R. Zimbelman et al. (2002), *EOS, 83, Abstracts Fall AGU, P71B-0457, F831*. [7] M.N. Peitersen et al. (2003), *man. in prep. for sub. to Icarus*. [8] T.K.P Gregg,, and S.E.H. Sakimoto,, (2000), *LPS XXXI* Abs. #1758. [9] S.E.H. Sakimoto and T.K.P. Gregg, (2001), J. Geophys. Res.106, 8629-8644. [10] J.R. Zimbelman et al. (2003), *LPS XXXIV,* Abs. #1387.[11] M.N. Peitersen (1999), *University of Pittsburg*, 394 pp. [12] M.N. Peitersen and D.A. Crown (1999), *JGR, 103,* 27,503-27516. [13] M.N. Peitersen and D.A. Crown (2000), *JGR, 105,* 4123-4134. [14] M.N. Peitersen and D.A. Crown (2003), *man. in prep for sub. to J. Geophys. Res.*. [15] J.R. Zimbelman (1985), *J. Geophys. Res. 90*, D157-D162. [16] S.M. Baloga et al. (1998), *J. Geophys. Res. 103*, 5133-5142. [17] E.W. Wolfe et al. (1988), *U.S.G.S. Prof. Paper 1463*, 1-97.